Int. J. Electrochem. Sci., 14 **(2019)** 3465 – 3476, doi: 10.20964/2019.04.47

International Journal of
ELECTROCHEMICAL
SCIENCE
www.electrochemsci.org

Short Communication

Corrosion Behavior of Aluminum in Carbon Dioxide Aqueous Solution at 50 ºC

Daoyu Li[1], *Zhen Shi*[2], *Huaping Xu*[1], *Yi Chen*[3], *Wenxin Feng*[1], *Zhiyuan Qiu*[1], *Hao Liu*[1], *Gang Lv*[1], *Shengping Wang*[2,*], *Youping Fan*[4]

[1] Guiyang Bureau, Extra High Voltage Power Transmission Company, China Southern Power Grid (CSG), Guiyang 550081, China
[2] Faculty of Material Science and Chemistry, China University of Geosciences, Wuhan 430074, China
[3] Operational Technology Department, Extra High Voltage Power Transmission Company, China Southern Power Grid (CSG), Guangzhou 510663, China
[4] School of Electrical Engineering, Wuhan University, Wuhan 430072, China
[*]E-mail: spwang@cug.edu.cn

Received: 15 January 2019 / *Accepted:* 14 February 2019 / *Published:* 10 March 2019

In this work, the corrosion behavior of aluminum in carbon dioxide solutions with different concentrations at high temperature (50 ºC) was studied. The corrosion of aluminum in the carbon dioxide solutions was inhibited to a certain extent compared to the corrosion in deionized water. It was found that an aluminum electrode in 0.84 μmol L^{-1} carbon dioxide solution with pH 4.35 had the lowest corrosion rate as observed from its lowest corrosion current, the most positive corrosion potential, and the maximum charge transfer impedance. The mechanism for aluminum corrosion inhibition was that HCO_3^- generated by carbon dioxide ionization developed an ordered charge field on the aluminum surface, shielding the diffusion of aluminum ions and inhibiting the dissolution of the oxide film on the aluminum surface. SEM, EDS and XRD confirmed that the corrosion products covering the surface of the aluminum electrode were $Al(OH)_3$ and/or Al_2O_3. Based on the above, it was elucidated that the Pt grading electrodes of the high voltage direct current (HVDC) valve cooling system lower the scaling rate in solutions with a certain concentration of carbon dioxide, and it was shown that the concentration of aluminum ions in the inner cooling water is a crucial factor affecting the scaling of grading electrodes. Therefore, reducing the concentration of aluminum ions in the inner cooling water, in other words, inhibiting the corrosion of aluminum, is the fundamental means for solving the scaling problem of the grading electrode. This paper will contribute to the research on production improvement techniques used for HVDC valve cooling systems.

Keywords: Aluminum, Corrosion, Carbon dioxide solution, Bicarbonate radical, Radiator, Thyristor, High voltage direct current

1. INTRODUCTION

High voltage direct current (HVDC) transmission systems have become the preferred resource allocation and long distance power transportation method due to their narrow transmission corridor, high transmission efficiency, and low power consumption [1, 2]. Unfortunately, the scaling of grading electrodes in deionized water cooling circuits of HVDC power transmission modules is a long-known and unsolved problem that has a great impact on the safe operation of the HVDC transmission system. Deionized water is used as the cooling water circulating in the in-valve cooling system, and its working temperature is in the range of 48-52 ºC. Grading electrodes are cylindrical bright platinum electrodes with deposition of mixed aluminum oxides and hydroxides (alumina) [3, 4]. The aluminum element in the deposition is derived from corrosion of the aluminum radiator and is precipitated on the surface of the grading electrodes under appropriate conditions. To solve the scaling problem of the grading electrode, it is necessary to suppress the corrosion behavior of the aluminum radiator in the in-valve cooling water system [5]. Previous reports have focused on the corrosion characteristics of aluminum in weak acid media (hydrochloric acid, sulfuric acid) [6, 7], aqueous alkaline solutions [8, 9] and neutral dilute salt solutions (for instance, halide media [10, 11] and sodium sulfate solution [12]).

According to the studies by Weber [13] and Siemen [14], the introduction of a certain concentration of carbon dioxide in the deionized water at 25 ºC lowered the scaling rate of grading electrodes. However, they did not identify the origin for the lowering of the grading electrode scaling rate. The scaling on the surface of the grading electrode is due to aluminum deposition, indicating that the corrosion behavior of the aluminum radiator in the inner cooling water system was suppressed when the scaling rate was lowered. This paper discusses the electrochemical corrosion behavior of aluminum in different concentrations of carbon dioxide aqueous solution at 50 ºC in order to elucidate the corrosion mechanisms, providing guidance for solving the scaling problem of the grading electrode in the HVDC valve cooling system.

2. EXPERIMENTAL SECTION

2.1. Electrochemical system

An electrochemical system for testing consisted of a working electrode, a reference electrode, a counter electrode and an electrolyte. Platinum black electrodes were used as the counter electrodes, and saturated calomel electrodes (SCE) were used as the reference electrodes. The SCE potential at 50 ºC is 0.228 V (relative to the standard hydrogen electrode (SHE)). The working electrodes were cut from the aluminum radiator with a 1 cm × 1 cm working surface. The model 3003 aluminum electrode was used [15] that was composed of Si (0.57 wt%), Fe (0.63 wt%), Cu (0.14 wt%), Mn (1.27 wt%), Zn (0.09 wt%), Li (0.03 wt%) and Al (97.31wt%). All of the surfaces other than the 1 cm^2 working surface were coated with epoxy resin. Prior to testing, the working electrodes were polished with diamond paper and nano-alumina powder, cleaned with deionized water and absolute ethanol, and dried and immersed in the testing electrolytes for 24 h.

Different concentrations of carbon dioxide electrolyte were prepared by the aeration method, and the concentration was controlled by different ventilation times. First, N_2 was injected into deionized water (100 mL) for 5 min (excluding the dissolved air in deionized water), and then CO_2 was injected into deionized water for 0, 10, 20, 30, 40, 50 and 60 min. Finally, all electrolytes were closed and left standing for 12 h. The concentrations of the carbon dioxide solutions were tested according to the ISO 925-1997 standard [16]. An S470 pH meter was used to test the pH of the electrolytes.

2.2. Electrochemical Test

Steady state polarization curves and electrochemical impedance spectroscopy (EIS) spectra were obtained using a CHI660D electrochemical workstation. The potential scan rate was 1 mV s^{-1}, and the potential range was 0.8 V (ranging from the potential 0.4 V lower than the stable potential to the potential 0.4 V higher than the stable potential). The corrosion potential and corrosion current density were obtained from the polarization curves.

The corrosion characteristics of the aluminum surface were determined from the results of EIS analysis that was performed over a frequency range from 1 Hz to 10^5 Hz with an amplitude of 5 mV. The electrolyte temperatures for all tests were between 48 and 52 ºC. During the testing, the electrochemical systems were kept in a shielding box.

2.3. Characterization

All of the SEM, EDS, and XRD test samples underwent accelerated corrosion by potentiostatic anodic oxidation for a more clear observation and analysis of the corrosion surface and corrosion products of aluminum. The anodization process used a two-electrode system with platinum as the cathode and an aluminum electrode after pre-treatment (polished, washed) as the anode. The stable potential (open circuit potential) at various concentrations was tested prior to the anodization. Based on the stable potential, the oxidation overpotential of 30 mV was increased to conduct accelerated corrosion experiments. The compositions of corrosion products were determined using a D8-Focus X-ray powder diffraction instrument with a Cu target. The scanning angle range was from 5 to 80 degrees, and the scan rate was 8° min^{-1}. SEM was performed using an SU8010 ultrahigh resolution field emission scanning electron microscope equipped with high performance X-ray energy dispersive spectroscopy (EDS).

3. RESULTS AND DISCUSSION

3.1. Different concentrations and pH of carbon dioxide solutions

The concentrations and pH of the carbon dioxide solution at different ventilation times are shown in Table 1. For 0-30 min, as the ventilation time increased, the concentration of the carbon dioxide solution gradually increased and the pH gradually decreased. Until the ventilation time of 40 min, the concentration and pH of the carbon dioxide solution tended to be stable, indicating that the prepared

carbon dioxide solution was near saturation. The concentration of HCO_3^- in the carbon dioxide solution was calculated according to formula (3), and the concentration of HCO_3 showed the same trend as the concentration of the carbon dioxide solution.

$$CO_2 + H_2O = H_2CO_3 \quad (1)$$

$$H_2CO_3 = H^+ + HCO_3^- \quad (2)$$

$$C(H^+) = C(HCO_3^{2-}) = \sqrt{C(CO_2)K_{a1}} \quad (3)$$

$$HCO_3^- = H^+ + CO_3^{2-} \quad (4)$$

Table 1. Concentration and pH of the carbon dioxide solution at different ventilation times

Ventilation time of carbon dioxide solution (min)	Concentration of carbon dioxide solution (μmol L^{-1})	pH	Calculated concentration of HCO_3^- in electrolytes (μmol L^{-1})
0	0	6.12	0.76
10	345	5.76	1.74
20	535	5.37	4.27
30	750	4.67	21.38
40	850	4.36	43.65
50	886	4.35	44.67
60	876	4.35	44.67

According to the ionization reactions (1), (2) and (4) of carbon dioxide in water, CO_2, H_2CO_3 molecules, and HCO_3^- and CO_3^{2-} ions are present in the carbon dioxide solution. For the study of the corrosion mechanisms of aluminum in the carbon dioxide solution, the CO_2 and H_2CO_3 molecules and the HCO_3^- and CO_3^{2-} ions in the carbon dioxide solution should be analyzed. Examination of the equilibrium ionization constants shows that the second-order ionization constant ($Ka_2 = 4.7 \times 10^{-11}$) of carbonic acid is far weaker than the first-order ionization constant ($Ka_1 = 4.7 \times 10^{-7}$). Thus, there are more HCO_3^- ions in the solution. Therefore, it is speculated that HCO_3^- ions play a major role in inhibiting aluminum corrosion in the carbon dioxide solution.

3.2. Polarization curves

The polarization curves of the aluminum electrodes are shown in Fig. 1. It is well known that the more positive the corrosion potential and the lower the corrosion current, the lower the aluminum corrosion rate [17, 18]. As the concentration of the carbon dioxide solution increased to 850 μmol L^{-1}, the corrosion potential of aluminum was gradually positively shifted, indicating that the corrosion of aluminum in the carbon dioxide solution was inhibited.

The data for the corrosion potential and the corrosion current density of the aluminum electrodes in the electrolytes are shown in Table 2. The corrosion current of aluminum in the carbon dioxide solution was lower than that in deionized water, indicating that the corrosion resistance of aluminum in the carbon dioxide solution was better than that in deionized water. The lowest corrosion current density and the

most positive corrosion potential of aluminum were measured in the 850 μmol L^{-1} carbon dioxide solution, indicating that the lowest corrosion rate of aluminum was obtained in the 850 μmol L^{-1} carbon dioxide solution. Thus, injection of CO_2 into deionized water can reduce the corrosion of aluminum.

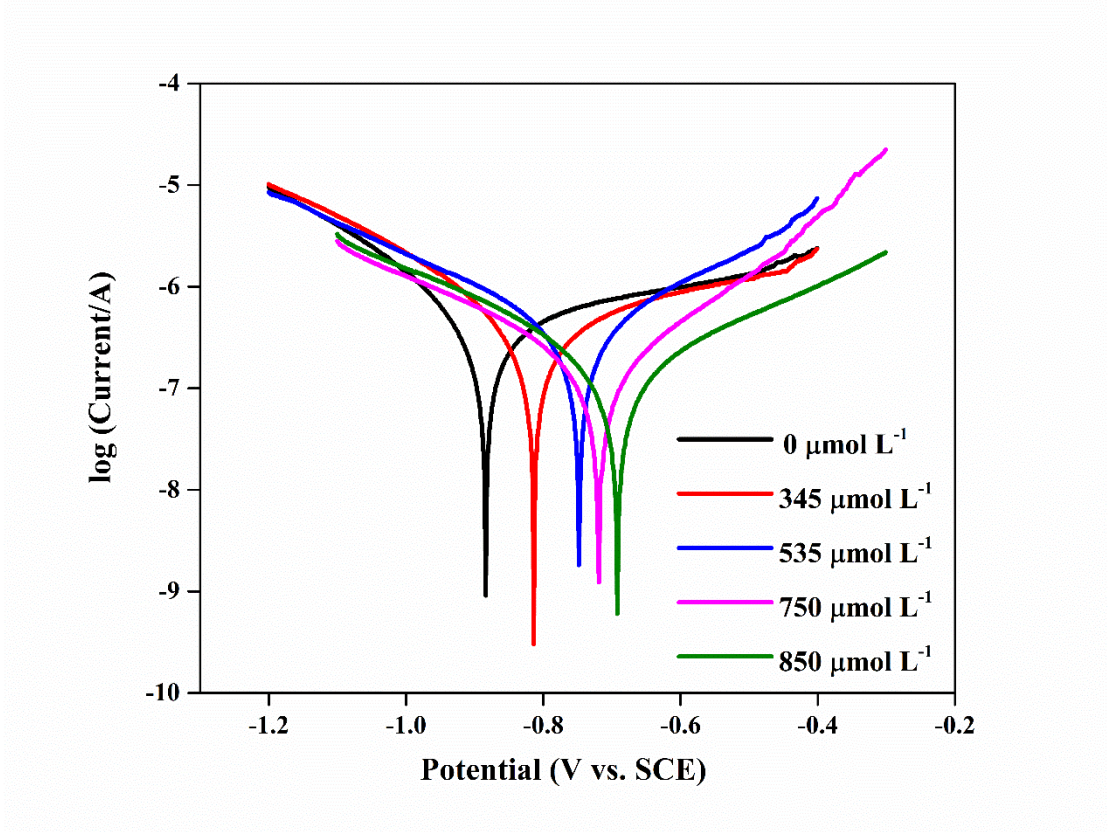

Figure 1. Polarization curves of aluminum in the carbon dioxide solution.

Table 2. Corrosion potential and current densities of aluminum in carbon dioxide solution at 50 ºC.

Concentration of carbon dioxide solution (μmol L^{-1})	Corrosion potential (V)	Corrosion current density (nA cm^{-2})	Anodic Tafel slope (V dec^{-1})	Cathodic Tafel slope (V dec^{-1})
0	-0.884	248.9	0.209	-0.124
345	-0.814	237.4	0.214	-0.145
535	-0.748	219.9	0.217	-0.221
750	-0.719	167.1	0.220	-0.272
850	-0.692	122.6	0.226	-0.195

3.3. EIS curves

According to the analysis of the surface state of the aluminum electrode, contributions from charge transfer impedance due to the oxidation of aluminum, diffusion impedance of ions in the electrolyte, impedance of the electric double layer capacitor, and impedance of the cladding layer should be present. The EIS curves of the aluminum electrode in carbon dioxide solutions with different concentrations are shown in Fig. 2a. The Nyquist diagrams of aluminum corrosion in carbon dioxide solutions with different concentrations show similar plots consisting of a semicircle and a straight line.

The physical meaning of the semicircle diameter in the high-frequency region is the charge transfer impedance (Rct) during the etching process, and the charge transfer impedance reflects the corrosion resistance of the aluminum in the solution. The lower the charge transfer impedance, the lower the aluminum corrosion resistance [19-21]. The equivalent circuit diagram of the electrochemical impedance spectrum is shown in Fig. 2c.

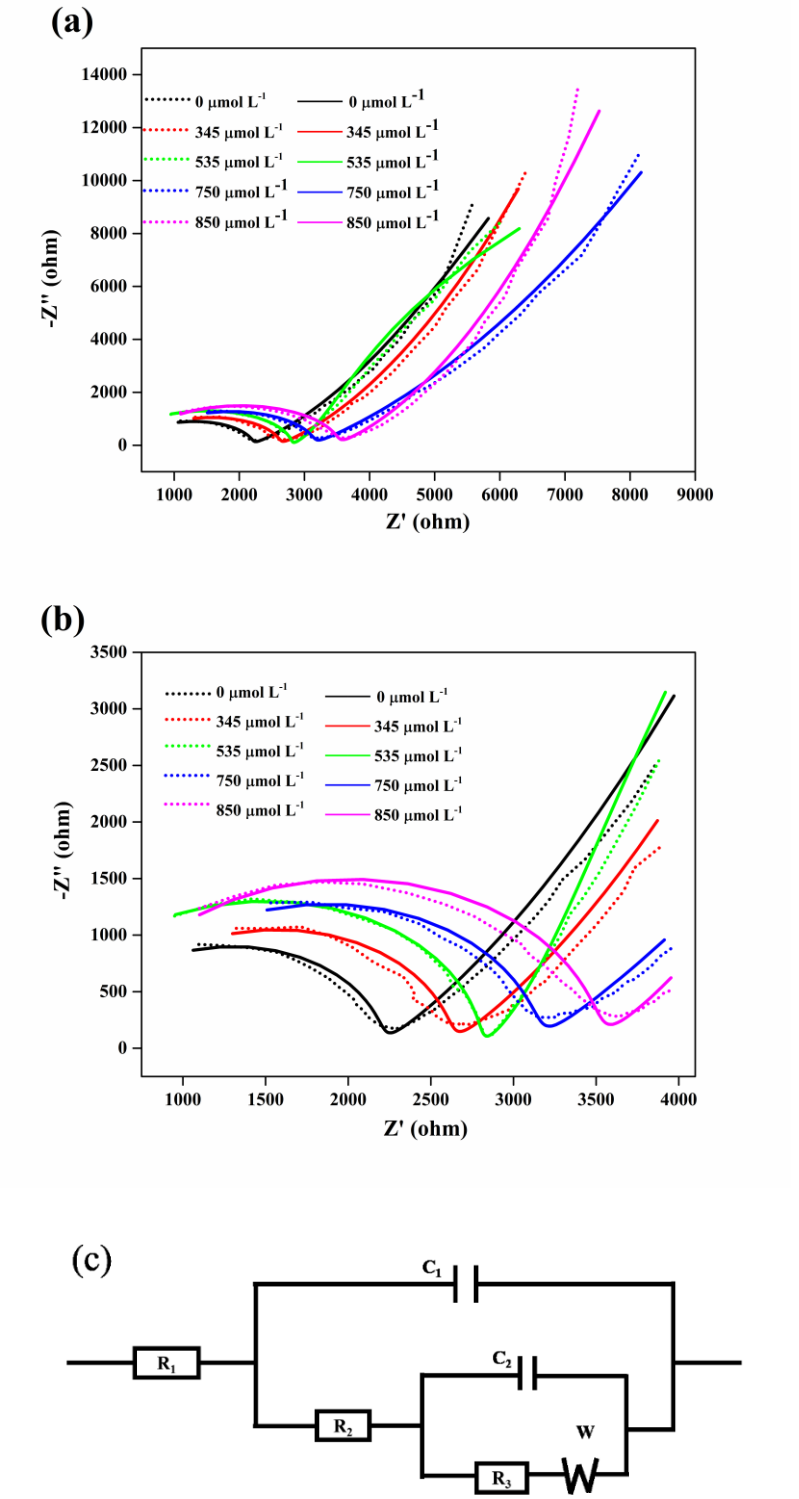

Figure 2. EIS curves (a), partially enlarged view of the curves (b), and their equivalent circuit model (c) for the aluminum electrodes in the carbon dioxide solutions at stable potential. The original data curves and the fitting curves are indicated by dotted and solid lines, respectively.

R_1 represents the resistance of the solution between the aluminum electrode and the reference electrode, R_2 represents the impedance of the electrolyte through the deposition layer, R_3 represents the charge transfer impedance for aluminum oxidation, C_1 represents the capacitance of the cladding layer, C_2 represents the capacitance of the double layer, and W represents the diffusion impedance of the ions in the electrolyte [22, 23].

Table 3. EIS parameters obtained by fitting the data to equivalent circuit model.

Concentration (μmol L^{-1})	R_1 (Ω)	R_2 (Ω)	R_3 (10^{-6}Ω)	C_1 (10^{-9}F）	C_2 (10^{-6}F)
0	753.0	1773	25.82	1.709	4.346
345	706.5	2064	30.26	1.464	4.865
535	639.9	2615	33.83	1.233	9.418
750	552.2	2825	38.79	1.168	2.249
850	273.3	3068	39.93	1.449	5.173

The data for the corresponding numerical simulations of the equivalent circuit are shown in Table 3. As the concentration of the carbon dioxide solution increased to 850 μmol L^{-1}, the charge transfer resistance gradually increases, indicating that the corrosion resistance of aluminum gradually increases and that the corrosion resistance of aluminum in the carbon dioxide solution was better than that in the deionized water. The highest charge transfer impedance was observed for the oxidation of aluminum in the 850 μmol L^{-1} carbon dioxide solution. This result was consistent with the results of the polarization curves shown in Fig. 1.

3.4. SEM and EDS

The surface morphologies of the aluminum electrode after corrosion in carbon dioxide solutions with different concentrations are shown in Fig. 3. Fig. 3b shows the presence of significant corrosion on the aluminum electrode surface in deionized water, with gullies, pores, and corrosion products observed. However, the corrosion of aluminum in the carbon dioxide solutions was relatively mild. Fig. 3c and 3d show that only small corrosion holes appeared on the electrode surface for the carbon dioxide solutions at the lower concentrations (345, 535 μmol L^{-1}). In Fig. 3e, and 3f, it is observed that the electrode surfaces were very smooth in the carbon dioxide solutions with higher concentrations (750, 850 μmol L^{-1}), and no obvious corrosion occurred.

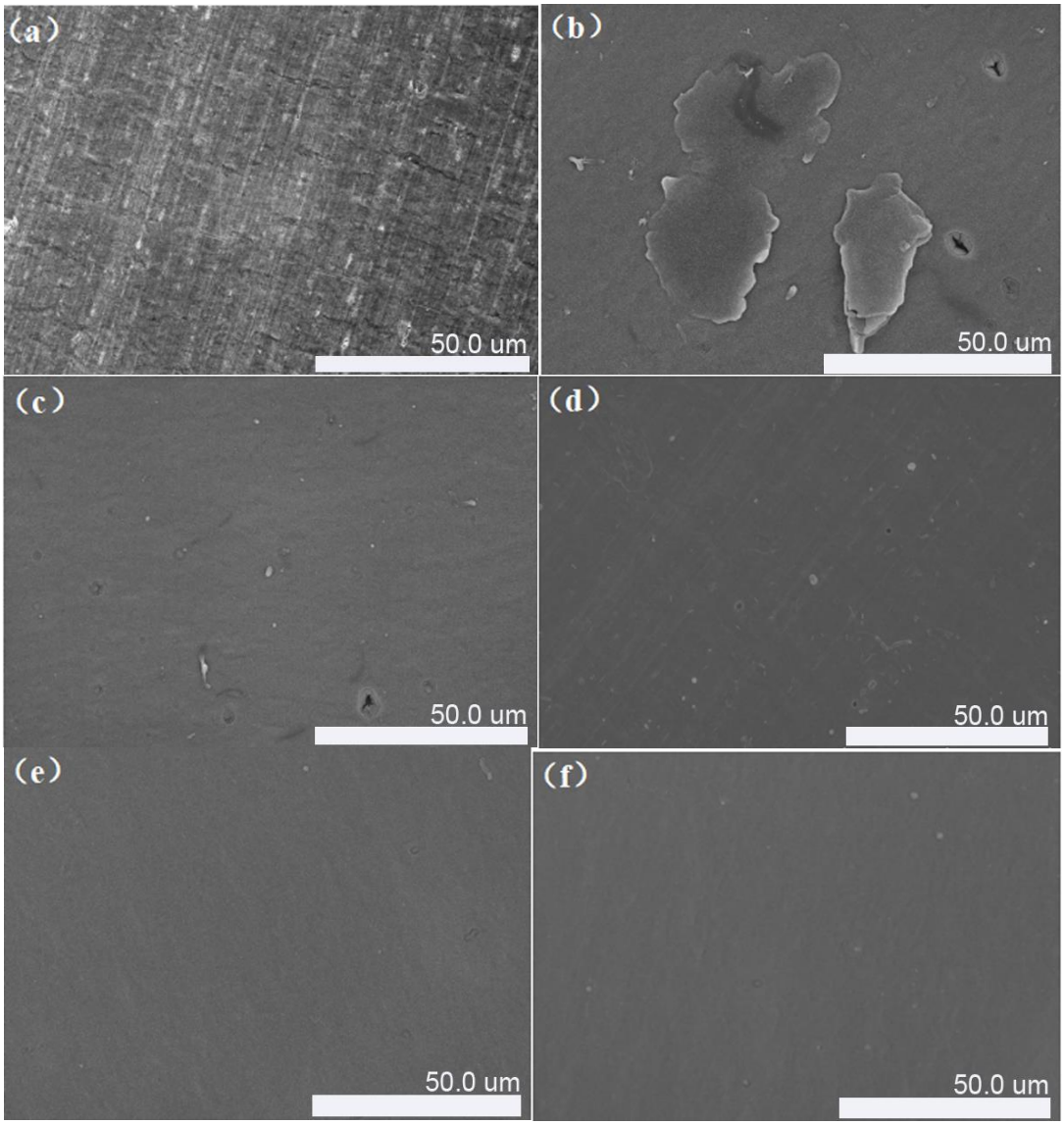

Figure 3. SEM images of the original aluminum (a) and the aluminum electrode surface in 0 μmol L^{-1} (b), 345 μmol L^{-1} (c), 535μmol L^{-1} (d), 750 μmol L^{-1} (e) , and 850 μmol L^{-1} (f) carbon dioxide solution.

The SEM and EDS of the corrosion products of the aluminum electrode in deionized water and in the 850 μmol L^{-1} carbon dioxide solution are shown in Fig. 4. It is observed from Figs. 4a and 4e that the corrosion of aluminum in deionized water was more severe and that more holes appeared. According to the EDS elemental diagram, the distributions of elements for the corrosion products in deionized water and in the 850 μmol L^{-1} carbon dioxide solution were similar. Aluminum was uniformly distributed on the electrode surface, while oxygen was mainly concentrated in the corrosion products. The elemental contents of the corrosion products of the aluminum electrode in deionized water and in the 850 μmol L^{-1} carbon dioxide solution are shown in Table 4. It was found that the corrosion products consisted mainly of aluminum and oxygen. The corrosion products of the aluminum electrode in deionized water and in the carbon dioxide solution should be consistent. The corrosion product of the aluminum electrode in the carbon dioxide solution did not develop either aluminum carbonate or aluminum hydrogen carbonate.

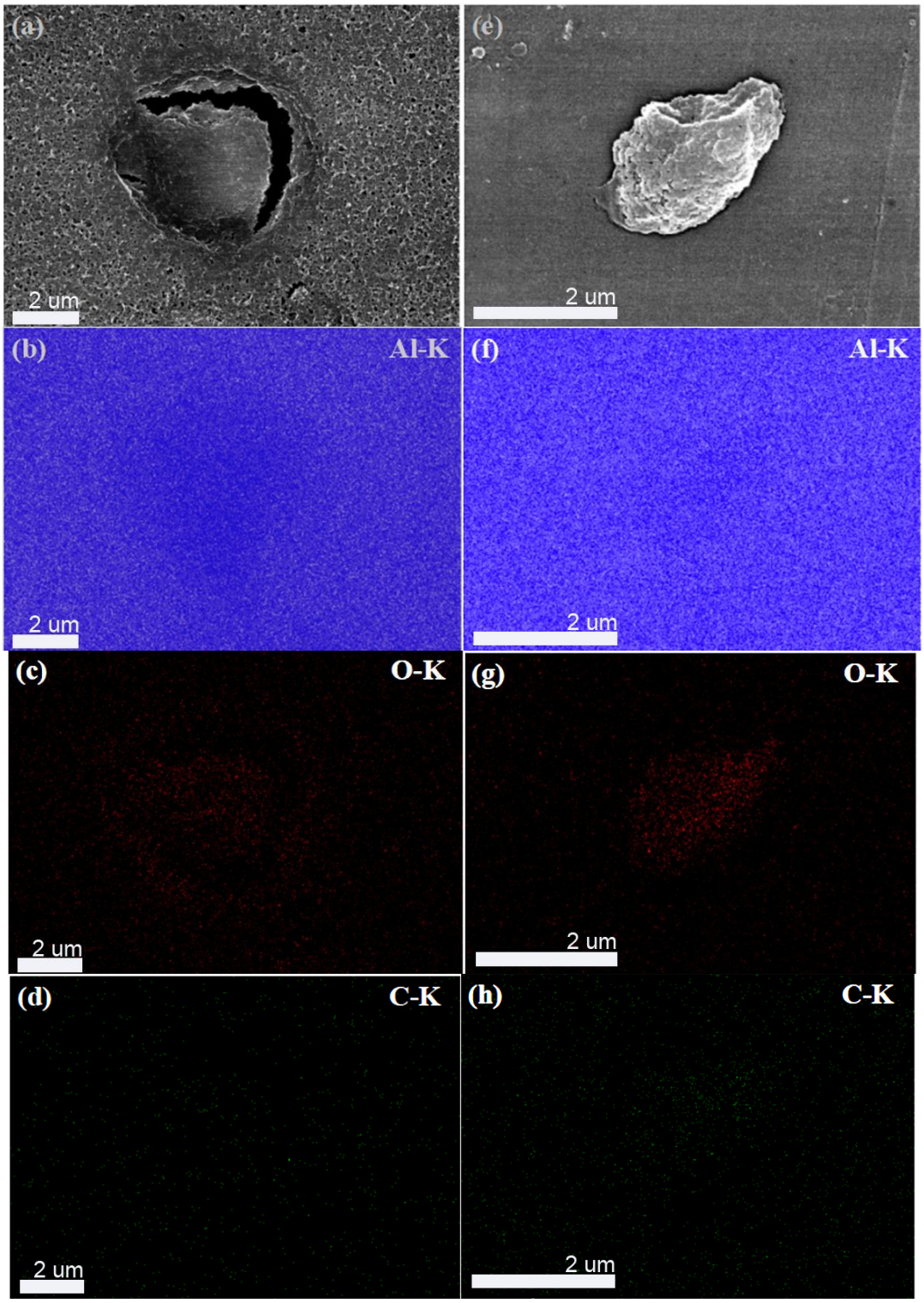

Figure 4. SEM images (a) and Al (b), O (c) and C (d) of EDS elemental analysis for corrosion products of aluminum in 0 μmol L^{-1} carbon dioxide solution, and SEM images (e) and Al (f), O (g) and C (h) of EDS elemental analysis for the corrosion products of aluminum in the 850 μmol L^{-1} carbon dioxide solution.

Table 4. Elemental contents obtained from the EDS analysis results presented in Figure 4.

Concentration of carbon dioxide solution (μmol L^{-1})	Al-K		O-K		C-K	
	Wt%	*At%*	*Wt%*	*At%*	*Wt%*	*At%*
0	84.51	75.35	12.63	18.90	2.86	5.72
850	86.36	77.10	11.53	18.31	2.11	4.59

3.5. XRD

The XRD spectra of the corrosion products of the aluminum electrodes in carbon dioxide solutions with different concentrations are shown in Fig. 5. For all of the samples, four strong peaks are observed at 39°, 45°, 65°, and 78° that match well to Al (PDF#040-708). Two strong peaks observed at 25° and 63° also correspond well to $Al(OH)_3$(PDF#26-0025) and Al_2O_3 (PDF#33-0018), respectively. This indicates that the corrosion products of aluminum electrodes in the carbon dioxide solutions and the deionized water contained $Al(OH)_3$ and Al_2O_3. This was consistent with the corrosion products of aluminum in moist air [24, 25]. As the concentration of the carbon dioxide solution increased, the peaks of the $Al(OH)_3$ and Al_2O_3 corrosion products at 25° and 63° gradually weakened. The peak of the corrosion product in the 850 μmol L^{-1} carbon dioxide solution almost disappeared. This indicated that the corrosion resistance of aluminum in the carbon dioxide solution was better than that in deionized water and that the lowest corrosion rate of aluminum was obtained in the 850 μmol L^{-1} carbon dioxide solution.

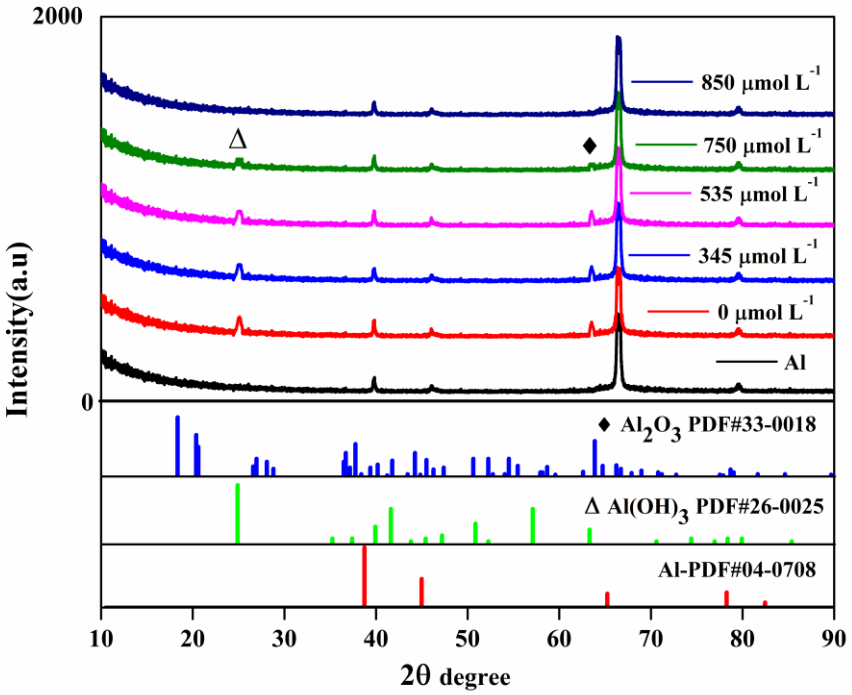

Figure 5. XRD spectrum of the corrosion products on the aluminum surface in the carbon dioxide solution.

3.6. Corrosion mechanism

It is speculated that HCO_3^- ions play a major role in inhibiting aluminum corrosion in carbon dioxide solutions. This paper mainly explores the origin for the inhibition of aluminum corrosion by HCO_3^- ions.

According to the work of Lashgari [26], the following processes are involved in the aluminum corrosion phenomena: damage of oxide/passive film (hydroxylation process) [27, 28], anodic metallic dissolution, and proton reduction. The oxide films are often chemically unstable in aqueous media and dissolve gradually through the interaction with water molecules, corresponding to the so-called hydroxylation process. At the interface region, some particular anions such as Cl^- [29, 30] can facilitate the hydroxylation process at the high energy surface active sites. However, HCO_3^- anion is relatively large and is adsorbed at a long distance and brings fewer water molecules onto the surface-active sites. Therefore, HCO_3^- ions inhibit aluminum corrosion based on suppressing the dissolution of the oxide film on the aluminum surface.

In the carbon dioxide electrolyte, HCO_3^- generated by carbon dioxide ionization adsorbed on the aluminum surface, eliminating the electric field on the original Al surface. The layer of bicarbonate HCO_3^- becomes electrostatically repulsive, reversing the charge in the oxide film layer for OH^-, which will suppress the deposition of aluminum on the surface. HCO_3^- continuously gathers on the surface of the electrode to form a shielding layer, shielding the diffusion of aluminum ions in solution. The Al^{3+} of the Helmholtz layer and the aluminum electrodes reach equilibrium of dissolution-precipitation. Because the continuous dissolution of aluminum is suppressed, aluminum corrosion is also suppressed.

4. CONCLUSIONS

The corrosion behavior of aluminum in weakly acidic carbon dioxide solution was studied. The electrolyte was simulated according to the working conditions of HVDC. The corrosion environment of aluminium was also special, such as high temperature, low conductivity and so on. Aluminum corrosion under these specific conditions was rarely reported. The results showed that compared to deionized water, the corrosion of aluminum in the carbon dioxide solution was suppressed. It was found that an aluminum electrode in the 0.84 μmol L^{-1} carbon dioxide solution with pH 4.35 had the lowest corrosion rate as observed from its lowest corrosion current, the most positive corrosion potential, and the maximum charge transfer impedance. It was confirmed that HCO_3^- plays a major role in inhibiting aluminum corrosion in carbon dioxide solutions. HCO_3^- inhibited aluminum corrosion by inhibiting the dissolution of the oxide film on the aluminum surface and by electrostatic repulsion of OH^- in solution.

This report focused on the primary reason for the grading electrodes scaling in HVDC valve cooling systems. It was elucidated that reducing the concentration of aluminum ions in the inner cooling water, in other words, inhibiting the corrosion of aluminum, is the fundamental means for solving the scaling problem of the grading electrode. This paper will provide guidance for the future application of aluminum in HCDC systems.

ACKNOWLEDGMENTS
This work was supported by the Programs of the China Southern Power Grid (CGYKJXM20180394, CGYKJXM20160094).

References

1. A. Kalair, N. Abas and N. Khan, *Renew. Sust. Energ. Rev.*, 59 (2016) 1653.
2. B.V. Eeckhout, D.V. Hertem and M.Reza, *Int. T. Electr. Energ.,* 20 (2010) 661.
3. H.Y. Qian, Y.Y. Zhou and W.C. Xu, *Adv. Mater. Res.*, 354 (2012) 1157.
4. Y. Wang, Z. Hao and R. Lin, *High. Voltage. Eng.*, 32 (2006) 80.
5. D.Y. Li, Y.X. Shi, H.P. Xu, Y. Chen, P. Zhou, X.W. Li, W.X. Feng and S.P. Wang, *Int. J. Electrochem. Sci.*, 13 (2018) 9346.
6. J.P. Dasquet, D. Caillard and E. Conforto, *Thin Solid Films*, 371 (2000) 183.
7. I.V. Aoki ,M.C. Bernard and C.D. Torresi, *Electrochim. Acta*, 46 (2002) 1871.
8. J. Zhang, M. Klasky and B.C. Letellier, *J. Nucl. Mater.*, 384 (2009) 175.
9. M. Lashgari and A.M. Malek, *Electrochim. Acta*, 55 (2010) 5253.
10. Z. Bo, L. Ying and F. Wang, *Corros. Sci.*, 51 (2009) 268.
11. E. Mccafferty, *Corros. Sci.*, 45 (2003) 1421.
12. S.G. Wang, H.J. Huang, M. Sun,K. Long and Z.D. Zhang, *J. Phy. Chem. C*, 119 (2015).
13. I. Weber, B. Mallick, M. Schild, S. Kareth, R. Puchta and E.R. Van, *Chem. Eur. J.*, 20 (2015) 12091.
14. P.O. Jackson, B. Abrahamsson and D. Gustavsson, *IEEE. T. Power. Deli.*, 12 (1997) 1049.
15. C.Y. Kong, R.C. Soar and P.M. Dickens, *J. Mater. Process. Technol.*, 146 (2004) 181.
16. Solid mineral fuels determination of carbonate carbon content gravimetric method, *ISO 925-1997*.
17. S.M. Moon and S.I. Pyun, *Corros. Sci*, 39 (1997) 399.
18. M.A. Amin, S.S. Abd El Rehim and A.S. El Lithy, *Corros. Sci.*, 52 (2010) 3099.
19. S.I. Pyun and S.M. Moon, *J. Solid. State. Electrochem.*, 4 (2000) 267.
20. N.D. Nam, W.C. Kim and J.G. Kim, *Mater. Corros.*, 63 (2012) 1004.
21. B. Zhang, Y. Li and F.H. Wang, *Corros. Sci.*, 49 (2007) 2071.
22. M. Trueba, S.P. Trasatti and D.O. Flamini, *Corros. Sci.*, 63 (2012) 59.
23. J. Wysocka, S. Krakowiak and J. Ryl, *J. Electroanal. Chem.*, 778 (2016) 126.
24. G.S. Frankel, *J. Electrochem. Soc*., 29 (1998) 2186.
25. T.H. Nguyen and R.T. Foley, *J. Electrochem. Soc.*, 129 (1982) 27.
26. M. Lashgari, E. Kianpour and E. Mohammadi, *J. Mater. Eng. Perform*, 22 (2013) 3620.
27. P.J. Eng, T.P. Trainor, G.E. Brown, G.A. Waychunas, M. Newville, S.R. Sutton and M.L. Rivers, *Science*, 288 (2000) 1029.
28. E.J. Lee and S.I. Pyun, *Corros. Sci.*, 37 (1995) 157.
29. M. Lashgari, *Electrochim. Acta*, 56 (2011) 3322.
30. W.M. Carroll, M. Murphy and C.B. Berslin, *Corros. Sci.*, 34 (1993) 1495.